Track Reconstruction and Alignment for ATLAS Devices under Test

M. E. Nelson, University of Cambridge, United Kingdom

September 11, 2014

Abstract

The 5 GeV test-beam at the DESY, Hamburg, site has been used to produce particle hits on a set-up of six equally-spaced planes of Mimosa 26 sensors for different plane geometries (e.g. plane separations) and environments (magnetic field strengths) for the ATLAS group. This is the DATURA pixel set-up, referred to as EUDET. The data extracted has been used to develop a new algorithm which takes the hit data and reconstructs the original trajectory of the test-beam particles, and then uses this fitted track to align the EUDET planes. This procedure can be used to calibrate devices under test which can be placed in EUDET, along the test-beam trajectory. Track reconstruction was carried out using General Broken Lines, and track alignment using Millepede II: both pieces of software were developed at DESY. Using this new algorithm (iterative alignment), the effects that different magnetic fields and plane geometries have on alignment and track parameters have been studied.

The long-term effects of this study will be the development of new track-fitting and alignment algorithms which can be used to calibrate and align future detectors. In ATLAS, the detectors to be calibrated will be the pixel and strip detectors. These applications will come in the near future, in detector development for the high-luminosity LHC upgrade.

Acknowledgements

I wish to acknowledge the invaluable support and contributions in undertaking this project. Firstly, I thank my two supervisors, Dr. Igor Rubinskiy and Mr. Alexander Morton, for their guidance during my project. Specifically, I think Dr. Rubinskiy for his insight in to how my project fits in to the wider scheme of the ATLAS experiment. I am indebted to Mr. Morton for his extremely helpful advice on the General Broken Lines and pattern recognition processes which had to be put to extensive use in the project, and for many long and valuable conversations about the software implementation.

Project aside, I wish to thank everyone involved in the DESY Summer School for making my summer so enjoyable. Thanks go to my fellow summer students, for providing an excellent social side to complement the wonderful physics. Thanks also to my lecturers for their teaching and providing an enrichment of my understanding of the deeply fascinating topic that is High-Energy Physics. Special thanks to the Summer School organisers, Dr. Olaf Behnke and Dr. Doris Eckstein, for taking charge of the entire summer.

Special thanks to Надежда Сергеевна Чернявская, as promised!

Contents

1 Introduction

1.1 The ATLAS Pixel and Strip Detectors

The study of particle track reconstruction is central to the ATLAS pixel and strip detectors. For particle trajectories within the pixel and strip detectors, as for any detector, it is important to have a system in place which allows for the complete reconstruction of these trajectories. It is also crucial to ensure that these trajectories are correctly aligned to provide a check that such a detector is correctly calibrated. The basis of high-energy physics measurements rests on these reconstructions and alignments of particle trajectories.

The ATLAS pixel detector is responsible for high granuality and high precision measurements as close to the proton-antiproton interaction of the LHC as possible. The pixel detector measures over the full ATLAS acceptance, and provides detailed measurements which allow the Inner Detector to find short-lived particles, such as B-mesons[1]. The pixel detector is effectively a series of silicon wafers which scintillate when particles pass through, generating a signal.

The ATLAS strip detector is an example of a semiconductor detector system. Strip detectors also rely on silicon. The detector is effectively arrangements of strip implants, forming an array of silicon wafers. Each of these wafer strips is then connected to a charge sensitive amplifier in order to generate a one-dimensional image of an event passing through the strip sensor. Additional strips can be applied to the wafer backside in order to produce a two-dimensional image of an event. Fig. 1 gives a schematic for these pixel and strip detectors.

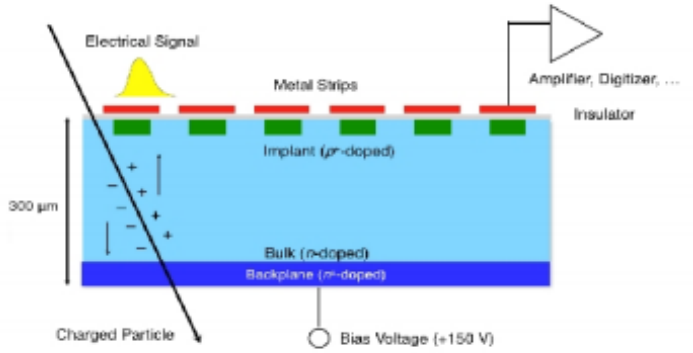

Figure 1: Strip sensor schematic, with an n-type bulk material with p-type implantations.The charged particle passes through the bulk, generating electron-hole pairs (excitons). The motion of these excitons in an applied electric field causes the sensor to behave as a semiconductor with the characteristic pn-junction.

When a particle passes through the silicon wafer, and into the implant, it ionises material in the detector. This ionisation generates electron-hole pairs in the implant material.The application of an electric field across the strip implant causes the system to behave as a pn-junction, so that the charge carriers drift to the electrodes at the opposite ends of the implant. The motion of these free exciton charge carriers then creates a signal which gives a measure of the initial exotic particle trajectory. This process is illustrated in Fig. 1 above.

1.2 Track Reconstruction and Alignment

The basis of my project is the track reconstruction and track alignment of trajectories formed from raw particle hits through a test-beam apparatus (the so-called EUDET, shown in Fig. 2). This set-up can contain a device under test to study. The specific devices under test can be the ATLAS pixel and strip detectors. Track alignment will be crucial for the calibration of future particle detectors in the high-luminosity LHC upgrade.

Figure 2: The sensor telescope used with the 5 GeV DESY testbeam. This telescope is based on the EUDET telescope and is called the DATURA pixel telescope. The device under test is placed at the centre of the system, with three sensor planes either side. Each plane contains a Mimosa 26 sensor, which is used to record the particle hit data.

Why is track reconstruction and alignment important here? The process of tracking allows for the determination of the properties of the charged particles in a detector. These include the type of particle, the particle trajectory, and the transverse momentum of the trajectory. This tracking is only possible because the particles interact with the detector via energy loss due to ionisation (given by the Bethe-Bloch formula). It is therefore clear that a good performance of the track reconstruction of raw data is key to the success of the physics programme within an experiment. A full track reconstruction is necessary for the determination of particle invariant masses and lifetimes. This track reconstruction is achieved in the ATLAS experimental group at DESY via the implementation of the General Broken Lines (GBL) software, which forms the basis of this report.

There are several challenges faced by tracking systems in LHC experiments. Important challenges are: the large momentum range in the particle trajectories (from MeV to GeV); the high-multiplicity of charged-particle events; the large backgrounds to consider; high data rates which are mitigated by effective data triggering; the large degrees of multiple scattering in the particle trajectories. The GBL software simulates accurately the effects of multiple scattering on the test-beam particle trajectories.

What is the central aim in detector alignment? Alignment is important because it provides an accurate description of the detector geometry, and hence provides accurate information on the spatial location of the detector modules. The Millepede II software is the procedure adopted by the DESY ATLAS group in determining the alignment parameters of particular devices under test. Track alignment is crucial to any high-energy

physics experiment. Alignment is necessary in order to ensure an high accuracy on precision measurements, such as precisions measurements on Z boson decay and B-meson tagging carried out by ATLAS.

This report focuses on the implementation of GBL in reconstructing the particle trajectories from raw data taken using the DESY test-beam through the EUDET set-up. Data exists for both no DUTs and DUTs present in the EUDET. Focus is also on the use of Millepede II to extract the alignment parameters for these detectors with the long-term goal of improved ATLAS detector quality for future ATLAS energy and luminosity upgrades.

1.3 Physics Requirements and the Project

The central physics requirements for the reconstruction and tracks and the track alignment are the limits on the errors in the raw data points. These are errors on individual hits and is calculated to be 5 microns. It is therefore necessary to align the tracks by determining track residuals (GBL track - particle hit data) with root-mean-square width of the order of 5 microns. Working with resolutions of orders higher than this would produce poor alignments.

This report first focuses on the test-beam set-up used to model the alignment of a real high-energy physics detector. This test-beam was generated at DESY and the set-up involved a set of planes which were misaligned so that alignments could then be applied to them, and hence residuals calculated. Focus then turns to describing in detail the software used to produce the track-fitted models from the raw data, and the software used to align the tracks with the particle hits on the planes. Together this procedure was referred to as Iterative Alignment. Finally results focus on the calculated track residuals from this Iterative alignment, using data with a magnetic field one and off. The χ^2 distributions for these tracks, and the subsequent problems with asymmetries in the alignment, is also considered and final conclusions on the track reconstruction and alignment algorithms applied are presented.

2 The Test-beam Set-up

2.1 EUDET and the Device Under Test (DUT)

An appropriate apparatus was devised in order to realistically simulate the motion of particles along an experimental beam line and the effects of beam materials on the trajectories of in-flight particles. The particular device under test (or DUT) was placed in the trajectory of a 5 GeV test beam of particles. The test-beam was located at DESY, Hamburg. The test beam settings could be varied to produce photon or electron beams.

A magnetic field could also be passed through the test-beam in order to generate helical particle trajectories.

How could the test beam, in the presence of a DUT, then be sampled at regular intervals? The most efficient solution was to construct sets of planes. The final set-up consisted of a total of six planes. The DUT (e.g. ATLAS pixel or strip sensor) was placed in the centre of the planes such that three planes were either side of the device. The plane spacing was set at 150 mm and could be adjusted. This combination of equidistant steel planes and the test-beam made up the EUDET apparatus. The set-up is presented in Fig. 3.

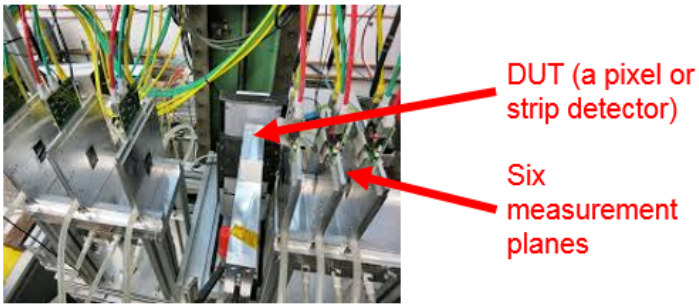

Figure 3: The DATURA pixel telescope in more detail. The measurement planes, with a DUT, are shown. This is the main telescope used at DESY, Hamburg. The test beam passes through the centre of the system, creating hits on the measurement planes. The EUDET software is then used to convert, cluster and form physical hits from the raw data. These hits shall form the basis of the particle trajectories which are to be reconstructed and used to align the six measurement planes in x, y and z.

At each plane in the EUDET the particle trajectories (from the test-beam) would produce sets of particle hits on the plane surface. These were the physical measurements from the beam. The EUDET therefore would produce six planes of raw data particle hits, but no tracks. This feature was important because it provided the means of using the plane set-up to align any DUT: the alignment of a DUT would be achieved by using software to properly align each of the individual planes. For this reason, the planes acted as 'sensor planes' which would initially be misaligned when hit data-taking began.

With the EUDET system in place the method of detector alignment was clear: all six sensor planes must be correctly aligned. It was necessary to first reconstruct the particle trajectories from the measured hits on the planes, and then apply a correct procedure that would align the planes based on a comparison of the reconstructed particle tracks with the measured particle hits. These two requirements were the essence of the General

Broken Lines (GBL) and Millepede II packages.

2.2 Local and Global Coordinates

In order to reconstruct particle tracks and align the sensor planes of EUDET, it is necessary to understand the geometry of the EUDET set-up. The geometries of the individual planes of hits and the complete detector frame must be understood separately. Two coordinate systems are required: these are the so-called local and global coordinates.

Local coordinates are defined in the reference frame of a particular plane. Each of the hit planes has independent set of three local coordinates, (u,v,w), about the centre of the plane. Any translations or rotations applied to the plane cause the local coordinates to translate and rotate in the same manner. (u,v,w) simply move with a particular plane.

Global coordinates are defined in the reference frame of the complete EUDET set-up. These coordinates are invariant under any translations or rotations of the plane and act as the coordinates of the laboratory frame of reference.

A third important system of coordinates are called pseudo-local. These are the two-dimensional coordinates, (x,y), which describe a particular hit position on a plane surface. These coordinates are necessary because any rotational or translational misalignments on a plane would cause the true positions of the measured hits, ($x + \Delta x$, $y + \Delta y$), to deviate from the expected hit positions, (x,y), which assumed no misalignment. The shifts in plane coordinates, (Δx, Δy), are related to the plane misalignments via a locally-defined Jacobian. It is necessary to explain the local and global parameters at work in the EUDET before discussing the Jacobians more fully. The geometrical relationship between the local and global systems is illustrated in Fig. 4.

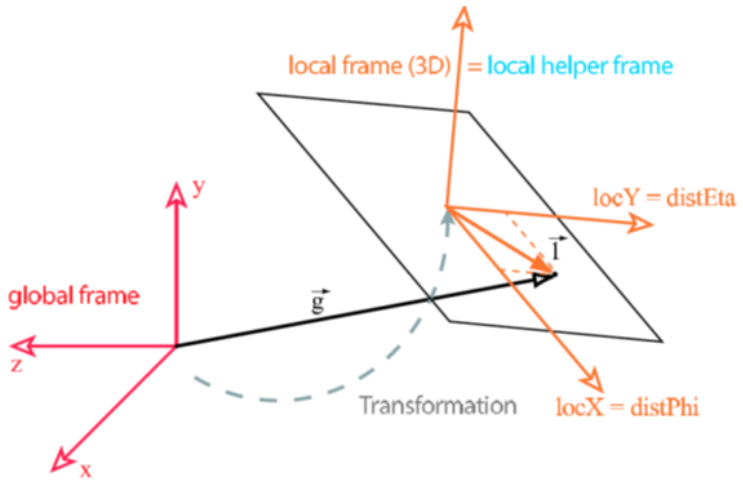

Figure 4: A visualisation of how the global coordinates in the detector frame of reference relate to the local coordinates which define a particular plane. The red system describes the global coordinates. These global coordinates are unchanged by any rotations or translations of the sensor planes. The orange system describes the local coordinates, which are defined at the centre of each separate plane. The two coordinate systems are related by a transformation matrix which is given by the product of three rotation matrices, each rotating in global x, y and z separately.

Local parameters are parameters which described single particle tracks which were incident on a particular plane. Across the six planes there are many thousands of local parameters to consider, including the positions of momenta of specific particle trajectories. Important local parameters to consider are the intercept and gradient of single particle trajectories at the point of interception of a sensor plane.

The global parameters are parameters which described the overall behaviour of tracks and planes in the laboratory frame of reference. These correspond to the six alignment parameters per plane: the three translations in x, y and z (global (x,y,z)) and rotations about the x, y and z -axis, denoted α ,β and γ respectively. Hence the global parameters are the alignment parameters, (Δx, Δy, Δz, $\Delta\alpha$, $\Delta\beta$, $\Delta\gamma$), for each of the planes. This gives a total of thirty-six alignment parameters. These are the alignment corrections computed by the Millepede II software.

2.3 Coordinate Transformations

Two important trasnformations can now be considered: 1) the use of Jacobians to transform from sensor plane misalignments to changes in the hit position defined in the pseudo-local coordinates; 2) the transformation between the local coordinates of an in-

dividual sensor plane and the global coordinates in the rest frame of the EUTelsecope set-up.

3 General Broken Lines (GBL)

3.1 GBL: an Overview

General Broken Lines [2] is an important piece of software, developed to provide models of the trajectories from from hits. GBL also incorporates the effects of multiple scattering on the particles as they propagate through the material in the set-up. GBL wis efficient and simple to interface with the Millepede software, which is used to align the track-fitted models with actuals data, or hits, on planes (see section 4). GBL accountes for this multiple scattering by constructing multiple thin scatterers between physical planes. These thin scatterers generate sets of 'kinks' in the model trajectory, leading to a broken lines track model.

At each of the planes, the GBL software defines two objects: a physical data point on the plane due to the interception of a true trajectory with the plane (a hit); and a state vector pointing out of the plane surface. GBL then constructes two thin scattering planes between these physical planes (modelling multiple scattering due to dead material in the detector), each with its associated state vector and zero hits. A scattering plane which models scattering due to silicon is also constrcuted and superposed on to each measurement plane. The broken lines trajectory is then formed by acting on the plane 0 state vector with a propagation Jacobian. This Jacobian propagates the state to the next plane, producing a new state vector there. Hence the trajectory is generated from the action of this propagation Jacobian matrix on state vectors. Connecting the different state vectors forms the GBL track. Fig. 5 shows the essential set-up of scattering and measurement planes in GBL. The Jacobians themselves are derived by considering the geometry of the test-beam system, working in general curvilinear coordinates. Working in curvilinear coordinates was necessary in order to account for future work with tilted sensors in the Telescope Pixel plane set-up.

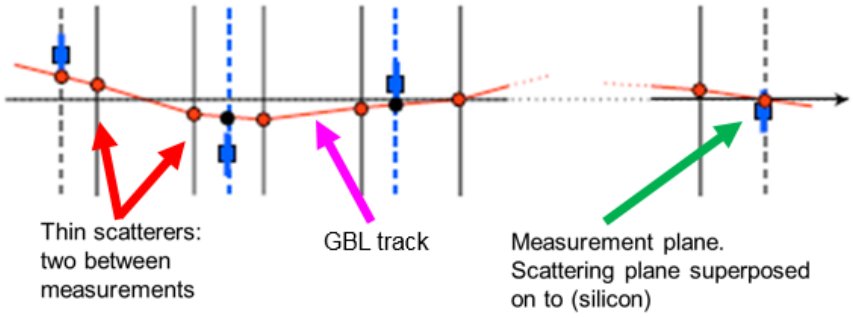

Figure 5: GBL works by constructing two scattering planes between each measurement plane. These scattering planes have an associated offset, which defines the spatial position of the state vector for that plane. GBL uses these offsets in its track reconstruction. The initial plane state vector is propagated to the next plane via the action of a propagation Jacobian. The state vectors are connected to up to form the broken lines track. Scattering planes are also superposed on to measurement planes in order to generate kinks in the track due to the scattering of the particles by the silicon on the Mimossa planes.

What made GBL such an appealing track-fitter to use was its use of offsets on scattering planes. An offset is the spatial position of a particular state vector on a scattering plane. By working with these offsets, GBL reduces the problem to the solution of a bordered band matrix. Such an entity is computationally simpler to solve, and hence extract the track parameters.

Several geometries were considered in the implementation on the GBL code calculation of the Jacobians, converting between local and global coordinates of the test-beam set-up.

3.2 The Mathematics of GBL

A flavour of the mathematics of the GBL algorithm is presented here. A more complete discription of this process is given in [2] and [3].

The mathematics of GBL is based on a χ^2 minimisation procedure which extracts the track parameters needed to fit a track to hits. An individual plane is decribed using the local coordinates (u,v,w), where w is perpendicular to the measurement plane. A track is described locally using the curvilinear coordinates, (x_c,y_c,z_c), which move with the track, where z_c is along the track direction and x_c is in the global (x,y) frame. At each thin scattered the two-dimensional offset, (u,v), is the fit parameter.

The variance of multiple scattering kinks, $\mathbf{V_k}$, is given by:

$$\mathbf{V}_k = \frac{\partial(u,v)}{\partial(x_c,y_c)} \begin{pmatrix} \theta_0^2 & \mathbf{0} \\ \mathbf{0} & \theta_0^2 \end{pmatrix} \left[\frac{\partial(u,v)}{\partial(x_c,y_c)}\right]^T = \frac{\theta_0^2}{(1-c_1^2-c_2^2)} \begin{pmatrix} \mathbf{1\text{-}c_2^2} & \mathbf{c}_1\mathbf{c}_2 \\ \mathbf{c}_1\mathbf{c}_2 & \mathbf{1\text{-}c_1^2} \end{pmatrix} (1)$$

Here the θ_0 matrix gives the variance in the curvilinear system, and the c_i are the projections of the offset directions of the local frame of each plane on to the track directions in the curvilinear frame.

A track may be defined locally with plane position $\mathbf{U}$ = (u,v), slope $\frac{\partial(u,v)}{\partial w}$ and inverse momentum, q/p, where q is the charge. GBL determines the track parameter corrections, and hence the kinks and associated errors, via a χ^2 minimisation. The χ^2 to minimise is:

$$\chi^2(\mathbf{x}) = \sum_{\mathbf{i=1}}^{\mathbf{n_{meas}}} (\mathbf{H_{mi}x} - \mathbf{m_i})\, \mathbf{V_{mi}^{-1}}\, (\mathbf{H_{mi}x} - \mathbf{m_i}) + \sum_{\mathbf{i=2}}^{\mathbf{n_{scat-1}}} (\mathbf{H_{ki}x} - \mathbf{k_{0i}})\, \mathbf{V_{ki}^{-1}}\, (\mathbf{H_{ki}x} - \mathbf{m_{0i}}) + (\mathbf{H_s x})^{\mathbf{T}}\, \mathbf{V_s^{-1}}\, (\mathbf{H_s x}) \quad (2)$$

Above $\mathbf{V_{mi}}$ and $\mathbf{V_{ki}}$ are the variances of the measurements and kinks respectively, whilst $\mathbf{H_{mi}}$ and $\mathbf{H_{ki}}$ are the respective matrices of the derivatives of the measurement and kinks with respect to the local and global parameters.

The special structure of the χ^2 solution matrix allows this matrix to be reduced to a bordered band matrix form. Bordered band matrices contain many null entries, and consequently are computationally simpler to invert in order to obtain the solution vector of the track parameter corrections.

3.3 Implementation of GBL

GBL and Millepede are implemented using the EUDET framework provided by the DESY ATLAS group to study devices under test in test-beam conditions. The full data analysis process runs in stages:

1) Converter: this converts raw data from each of the six sensors (i.e. the particle collisions on each sensor plane) in to a common computational language used by the EUDET, GBL and Millepede packages. This LCIO file structure is the language used throughout the analysis.

2) Clustering: this groups several pixels together, for each given plane. These are known as clusters. The scintillation at a particular pixel corresponds to at least a single particle. The maximum number of pixels scintillated due to a single particle is four, obtained from simple geometric considerations of square pixels in the ATLAS pixel detector.

3) Hitlocal: this process takes each of the separate clusters of hits and assigns a spatial position to each cluster. These spatial cluster measurements correspond to the actual data measurements of hits. Each hit is then defined with respect to the local coordinate system of the plane it existed on. 1) - 3) successfully generate the measured data as sets of hits on planes.

4) Track Search Helix: an important part of the analysis is the use of pattern recognition, carried out at this stage. Pattern recognition takes the generated hits and assigns a specific set of hits to a specific track. Once the hits are related to possible tracks it is then possible to actually construct these tracks using the GBL programme. To make the pattern recognition as efficient as possible it is important to include as many hits as possible whilst simultaneously minimising the noise and the misassociation of a particular hit with a particular track.

(Aside: the pattern recognition processes mentioned above can be described in more detail. To carry out pattern recognition, a state vector is seeded at a hit position on the very first plane in the set-up. This state vector is parameterised by an angle to a plane and a magnitude. The state is then propagated to the next plane using simple equations of motion. This propagated state will lie at some distance from an actual hit. This hit has a pre-defined acceptance: some radial area centred on the hit, typically 0.5 - 3 mm. If the state lies within the hit acceptance, then that state is assigned to that hit. If multiple states lie within the acceptance, then all states bar one are removed. This process is repeated across all planes, assigning hits to specific state vectors.)

5) GBL Track Fit: this is the GBL-based section of the procedure. This process takes as input the geometries of the six planes, stored in a gear file. The geometries contain the spatial positions of the planes, defined globally, along with the initial values of the six alignment parameters: the three spatial translations and the three angular rotations. The process generates GBL state vectors for the planes and outputs the GBL-fitted track models.

6) GBL Align: this subroutine interfaces with the Pede alignment procedure of Millepede II in order to accurately align the generated tracks by comparing the GBL fitted models with the measured hits. The motivation behind Millepede II and the alignment process is the focus of the next section. Parts 5) and 6) are ultimately combined in to one complete 'iterative alignment' procedure.

GBL functions from several important input, given in Fig. 6. Here the flow-process of GBL is presented.

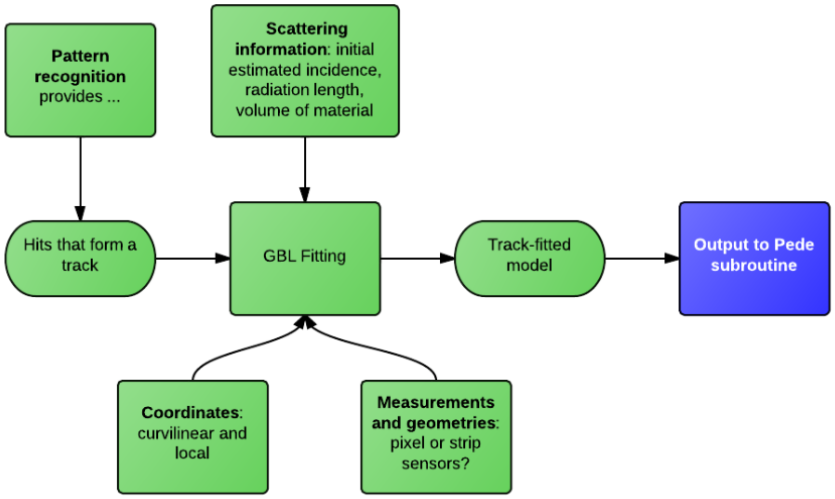

Figure 6: The basic inputs for GBL. GBL takes inputs from scattering information (material properties), coordinate frame to use (curvilinear coordinates for the propagation Jacobian and local coordinates for the alignment Jacobian, which is implemented in the Pede subroutine) and information about the geometry of the planes in the EUDET system. This geometry is stored in gear files and it includes the plane positions and any misalignments. The outputted plane information is stored as a gear file which is used as an input for the Pede subroutine. This performs the track alignments.

4 Millepede II

4.1 Millepede II: an Overview

The broken line tracks produced by GBL, which model the data trajectories through the six planes of the test-beam set-up, need to be correctly aligned. A true impact point on a particular plane is a physical measurement and corresponds to a hit. GBL track trajectories correspond to track models of the true particle trajectories producing the plane hits. The essence of alignment is just to minimise the weighted track residuals with respect to the track parameters. Fig. 7 provides a schematic of a typical alignment process.

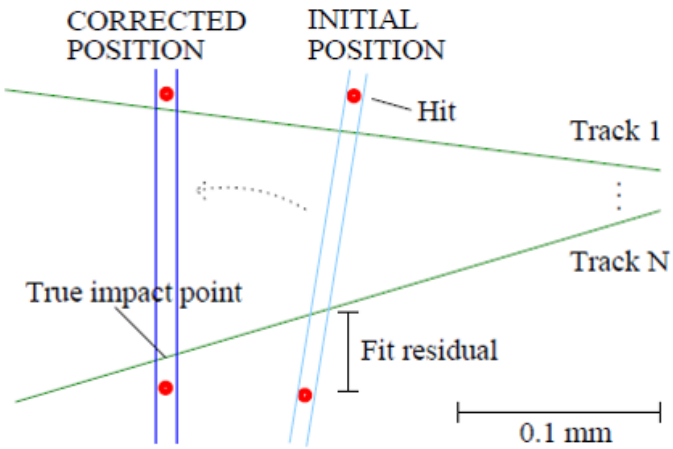

Figure 7: An example of a misalignment of the plane. For each separate track, Millepede computes the residuals of the measured hit - fitted-track interception. Millepede calculates the residuals all hits due to each separate track. It then looks at each of the N tracks in turn. These residuals are used to extract the alignment parameters which transform the plane from its initial position to its corrected position.

The Millepede II software[4] performs a reliable and fast alignment of the reconstructed broken line tracks from GBL. The Millepede alignment method is a computational solution to a least squares problem of many parameters: the thirty-six global parameters across the six planes in the test-beam set-up, and the many thousands of local parameters. Millepede solves this minimisation problem by simultaneously fitting the global and local parameters and taking all correlations in to account. The final solutions correspond to the global parameters only, and hence the required alignment parameters for the plane.

The χ^2 expression to be minimised with respect to the track parameters (local and global) in Millepede is (linearised to first order)[4], [5]:

$$\chi^2 = \sum_{j}^{tracks} \sum_{i}^{hits} \frac{1}{\sigma_{ij}^2} \left(\mathbf{m_{ij}} - \mathbf{p_{ij}}(\mathbf{g_0}, \mathbf{l_0}) - \frac{\partial \mathbf{p_{ij}}}{\partial \mathbf{g}} \mathbf{\Delta g} - \frac{\partial \mathbf{p_{ij}}}{\partial \mathbf{l_j}} \mathbf{\Delta l_j} \right)^2 \tag{3}$$

Here the summation is over all hits and tracks. Here σ_{ij} is the error on a particular hit, $\mathbf{m_{ij}}$ is a measurement, $\mathbf{p_{ij}}$ is the GBL fit and the remaining terms are first order corrections of local parameters ($\mathbf{l_j}$) and global parameters ($\mathbf{g}$). Such an expression produces a large matrix of thousands of entries which depend on both local and global parameters. The importance of Millepede is to implement a process that reduces this matrix to a much simpler form which could be inverted computationally economically, giving a solution vector containing only alignment corrections to the planes.The pre-decomposed

solution matrix is shown in Fig. 8.

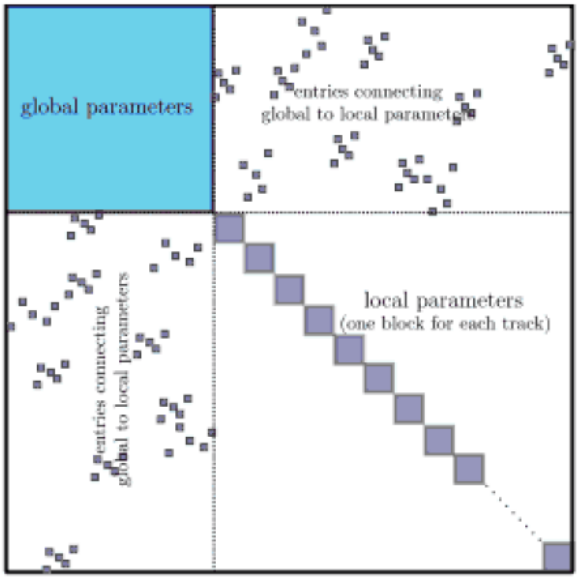

Figure 8: The basic form of the matrix generated from the chi-squared calculations in Millepede. This matrix has a special block form: some block components depend only on the global parameters, whilst others on the local parameters. The matrix decomposition reduces this matrix to a much smaller matrix which has matrix elements given in the global parameter block component.

4.2 The Mathematics of Millepede II

For a fuller description of the detailed mathematics of Millepede II, see [2], [4] and [5].

The expression (3) is minimised by taking differentials with respect to each of the parameters, producing a set of n + Nx equations, where n is the number of global parameters, x the number of local parameters and N the number of measurements of a particular local parameter over the six planes. Crucially, local parameters of one particular track are not dependent on the local parameters of any of the other tracks. Typically a given local parameter only depends on a small number of global track parameters. This property leads to a special structure in the χ^2 solution matrix (Fig. 9).

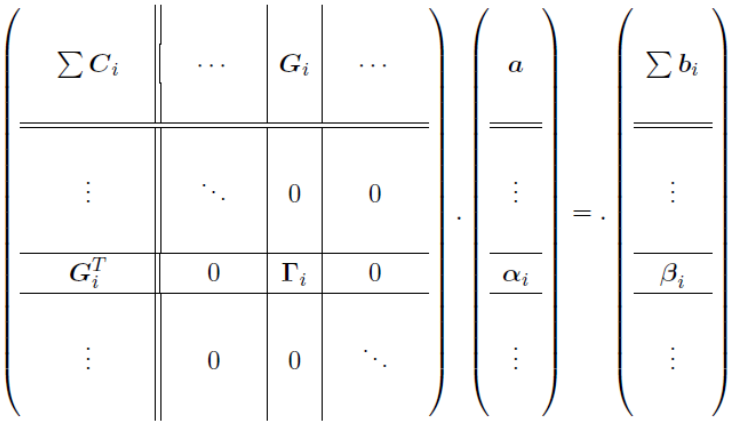

Figure 9: The full matrix equation which Millepede must solve. It first reduces the size of the block matrix to include only global parameters and then it inverts this matrix to extract the solution vector of only the global alignments. The C-blocks contain only the global parameter information, the Γ - blocks only local parameter information, whilst the G-blocks contain global and local parameter. The multiplying column vector contains the global and local parameters. The matrix is reduced to just the C-block which is multiplied by the vector of only a-elements, not a + α. The a-elements correspond to the global (alignment) parameters.

Millepede applies matrix reduction (via Cholesky decomposition[2]) to the block matrix in Fig. 9. This reduces the local parameter-dominated (n + Nx)× (n + Nx) normal matrix to a simpler n × n matrix which multiplied a column vector **a** of only global parameters. Matrix inversion then solves for this global parameter vector: the extracted thirty-six alignment parameters correspond to the corrections for the three rotations and translation for each plane. Such a significant matrix reduction is achieved without any need for an approximation.

Millepede also uses the feature of Lagrange multipliers to incorporate additional constraints in to a particular solution. This feature is not explored in the final analysis.

4.3 Implementation of Millepede II and Interative Alignment

The implementation of Millepede using the EUDET framework follows from the execution of GBLTrackFit and GBLAlign. The Millepede process runs from four key inputs for each particular measurement (i.e. hit):

1) The "hit - track model" residual.
2) The standard deviation of a particular hit.

3) The total number of local and global parameters required by the model.
4) The track model derivatives, separately with respect to a) local parameters and b) global parameters.

Millepede splits in to two processes: Mille and Pede. Mille acts as a subroutine for data acquisition and writing to binary files. Pede then takes each binary file, which contains the above four inputs, and runs the least squares process necessary to generate the alignment parameters.
The total procedure for pattern recognition, GBL track-fitting and Millepede alignment[6], [7] is combined in to one complete algorithm of iterative alignment. The alignment is iterative in the sense that track fitting and track alignment are carried out and then repeated in order to produce residuals as close to zero (perfectly aligned) as possible and to ensure that the χ^2 distributions for the track-fitting and the track alignments are normalised correctly. This is subject to the constraint of 5 microns on the track-fitting resolution (see 1.3). The procedure for iterative alignment is summarised in Fig. 10.

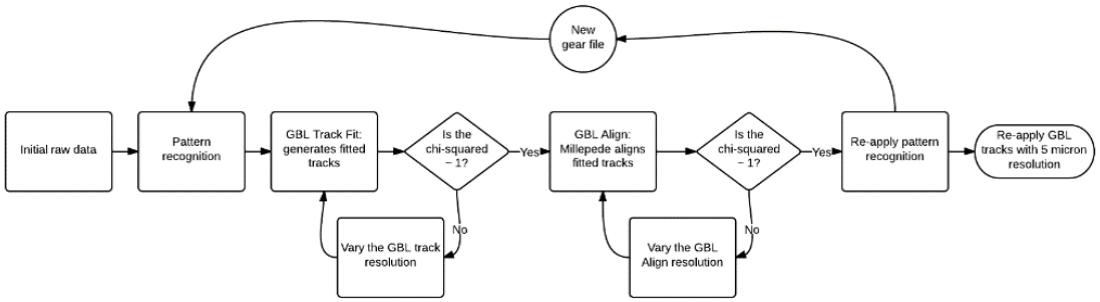

Figure 10: The flow process for iterative alignment. Pattern recognition is applied to the initial raw data, matching hits to tracks. This is then input in to GBL to produce fitted tracks. The chi-squared is then checked, If it is 1, then the tracks are outputted to Millepede for alignment. If not, then the errors on the plane positions and the hits are not properly accounted for and the reconstruction is repeated. The chi-squared is again checked after alignment. Following the production of the aligned tracks, pattern recognition is re-applied in order to generate a new gear file. If the track residuals produced at not properly aligned, then the entire process repeats using the newly-generated gear file containing the aligned plane geometries.

There are several motivations behind using iterative alignment. It is not possible to align the planes all at once due to the presence of weak modes in the system. These weak modes are small misalignments of the EUDET planes which introduce shifts in to the χ^2 distributions. Also tracks aligned after only one iteration are still poorly aligned because they are created out of misaligned data - the initial raw hit data. For this same

reason the pattern recognition is also poor if only a single iteration has been considered.

The application of the above processes builds up to the final results: the residuals for the GBL tracks pre- and post-alignment, for several different magnetic field conditions and for several different alignments. These alignments are the re-alignments due to the introduction of separate x and y-shifts and z-rotation misalignments to the EUDET planes.

5 Results and Analysis

Data for the GBL-fitted tracks before and after alignment has been obtained for the cases of 0 T and 1 T magnetic fields. Additionally, the residual and differential residuals (residual/error) have also been determined and compared. The pattern recognition analysis if first presented, in order to indicate that tests of pattern recognition have been made and the process validated.

5.1 Pattern Recognition Analysis

Pattern recognition, applied before the track reconstruction, has been validated by studying the detailed effects of different hit acceptances and magnetic fields on the average number of tracks produced from particle hits on planes in the EUDET.

Fig. 11 shows the relationship between the average number of tracks produced (a direct measure of the average number of hits) as the magnetic field through the set-up, for cases with 0 T, 0.5 T and 1 T fields. This has been plotted for four different hit acceptances: 3 mm, 2 mm, 1 mm and 0.5 mm. A hit acceptance of 3 mm corresponds to the acceptance region occupying 12.6 % of the total area of one pixel. A corresponding 0.35 % of area is occupied for a 0.5 mm acceptance.

Fig. 11 demonstrates that for smaller hit acceptances the average number of tracks produced falls. This is expected since, by decreasing the acceptance, the acceptance area in which a specific track is matched to a specific hit falls. Consequently the total number of tracks assigned to hits must also fall. This is the expected behaviour for pattern recognition.

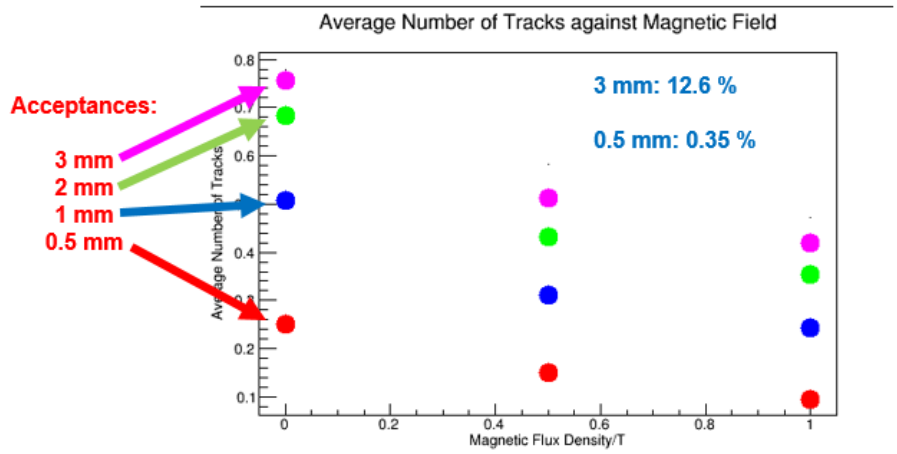

Figure 11: A plot of the average number of tracks matched by pattern recognition for different magnetic field strengths. The track number provides a measure of the number of hits assigned to a particular track. The relationships in this plot indicate that pattern recognition is behaving as expected for different magnetic fields and hit acceptances. This provided a good sanity check to ensure that hits were being assigned tracks in the correct way.

Conclusions drawn from Fig. 11 are that, in order to optimise the track-fitting, the number of shared hits must been minimised to zero. A shared hit occurs when more than one track lies within a hit acceptance region. If this happens, then all but one of the tracks must be dropped from the pattern recognition. It is also important to maximise the number of hits assigned to a particular track, in order to generate an accurate reconstructed track and to align the track well. The maximum number of hits per track implemented was six.

The plot also validates the expected behaviour of pattern recognition for different magnetic fields. Increasing the field strength causes the average number of tracks to fall. This is expected since a stronger field causes the hit trajectory to bend, so that the trajectory is no longer normally incident on particular plane. This then minimises how effectively hits can be matched to track in the pattern recognition.

With the pattern recognition procedure validated, it is now possible to consider track reconstruction and alignment.

5.2 GBL Tracks: Pre-Alignment

Fig. 12 shows a typical residual plot for the reconstructed tracks before alignment (via Millepede II) has been applied. The iterative alignment produces a total of 12 residual

plots: 6 for the x-residuals on each plane, and 6 for the y-residuals. The residuals are constructed by plotting the number of events against the residual value itself, where the residual is given by the separation of a hit and the corresponding GBL-fitted track.

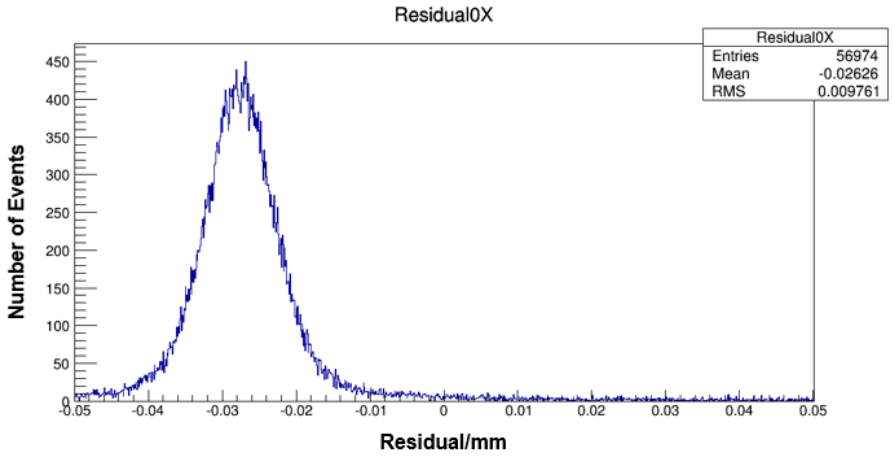

Figure 12: The residual in x for the 0th plane before alignment. The deviation from zero justifies the need to properly align the planes. The widths are a measure of the error on the hit positions.

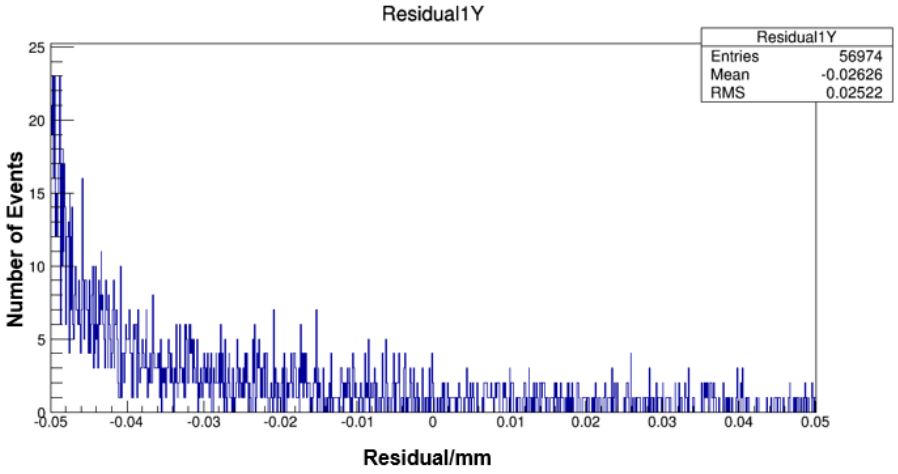

Figure 13: A corresponding residual in y for the 1st plane. The alignment here is even worse than for the case of x. This was a general feature: the y residuals were off-centred more than the x-residuals for pre-alignment. This indicates that the Mimosa planes are more sensitive to misalignments in the x-direction compared to misalignments in the y.

Fig. 12 gives the x-residual for plane 0 and Fig. 13 the y-residual for plane 1, in the case for zero magnetic field. These plots show clear misalignments: the deviation of the residual peak from the zero is due to initial plane misalignments in the EUDET system. The width of each residual is a measure of the error on a particular hit and plane. Performing alignments will help to centre of residual and reduce the plane error. It is expected that the root-mean-squared width should reduce to approximately 5 μm since this size corresponds to the intrinsic error on the position of a particular hit. Corresponding differential residuals have also been calculated. The differential residuals are residuals weighted by their respective errors.

Misalignments are also seen in the initial track-fits for B = 1 T field data, again due to the initial plane misalignments in the set-up. An example of such residuals is given in Fig. 14 below.

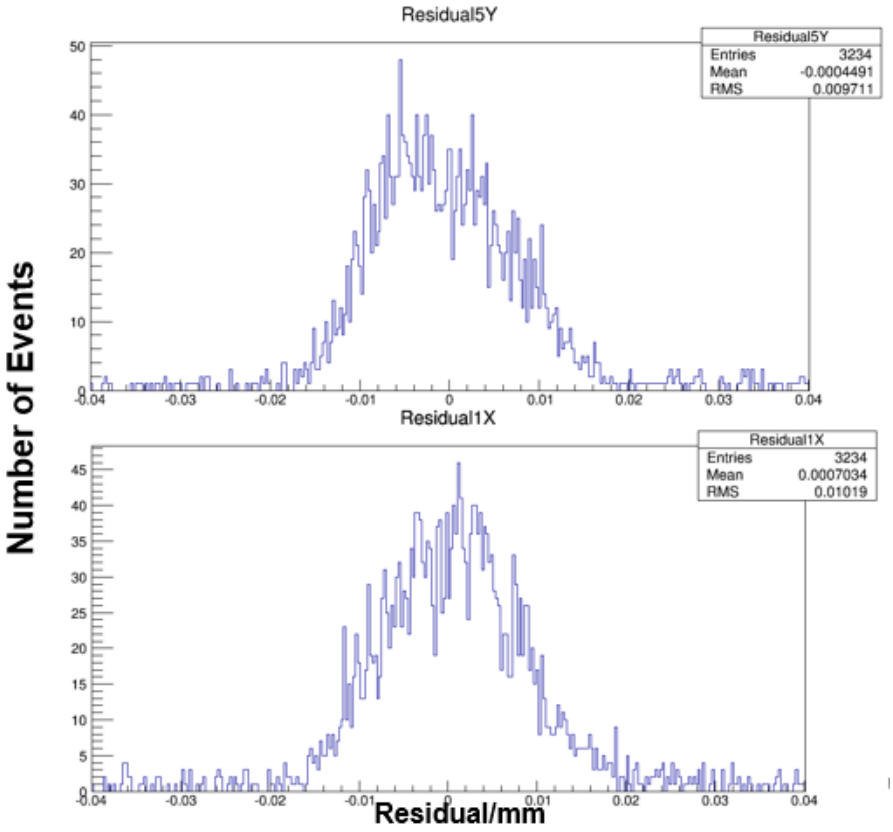

Figure 14: Example residuals for the 1 T data pre-alignment, looking at x-residuals on plane 5 and y on plane 1. The misalignments are not as prominent here compared with other data. The plots also show this characteristic peak structure that is sometimes seen in the data. The nature of these peaks is not well understood and will be discussed later.

A final important part of the analysis comes from the χ^2 distributions of the GBL-fitted tracks. Fig. 15, 16 and 17 gives the χ^2 distributions for 0 T, 0.5 T and 1 T data respectively. This is for the pre-aligned data. These distributions are central to testing the alignment process. The χ^2 distributions, weighted by the number of degrees of freedom, have a mean deviating from unity. These distributions take into account of residuals across all of the 6 planes, and the errors on each of the residuals. The mean value provides a goodness of fit comparison between the track-fitted model and the actual hit data. The strong deviation from unity in the mean indicates a severe misalignment of the planes. This supports the initial misalignments seen in the x and y-residuals. It is expected that the χ^2 will normalise correctly after alignment.

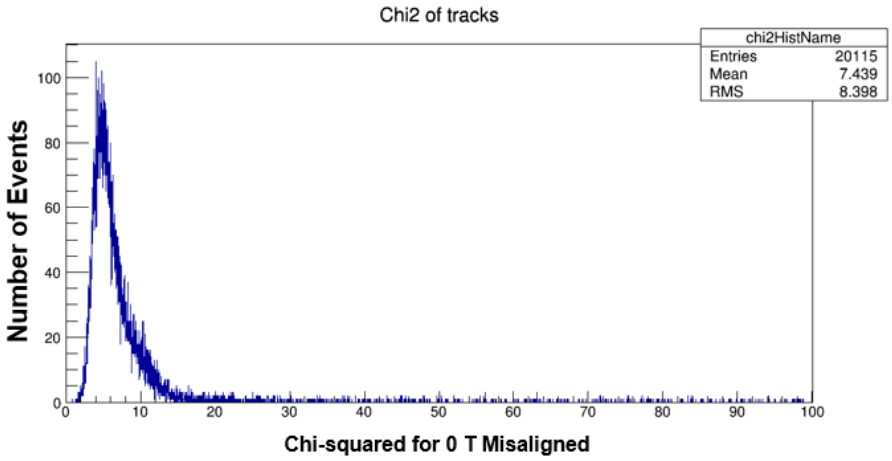

Figure 15: The χ^2 distribution for the 0 T data. The average value deviates far from unity, indicating that there is significant misalignment in the planes. This is expected for the GBL-fitted tracks prior to any alignment.

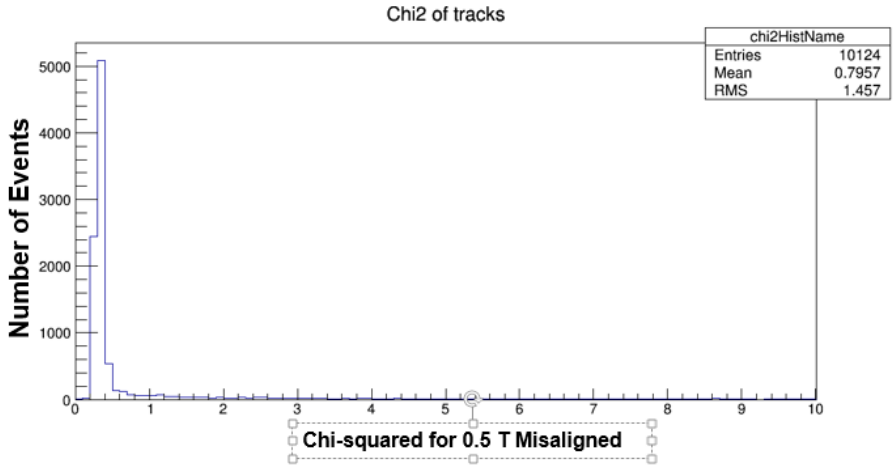

Figure 16: The corresponding χ^2 for the 0.5 T field data. This also show expected mean deviation for unity due to the misalignment.

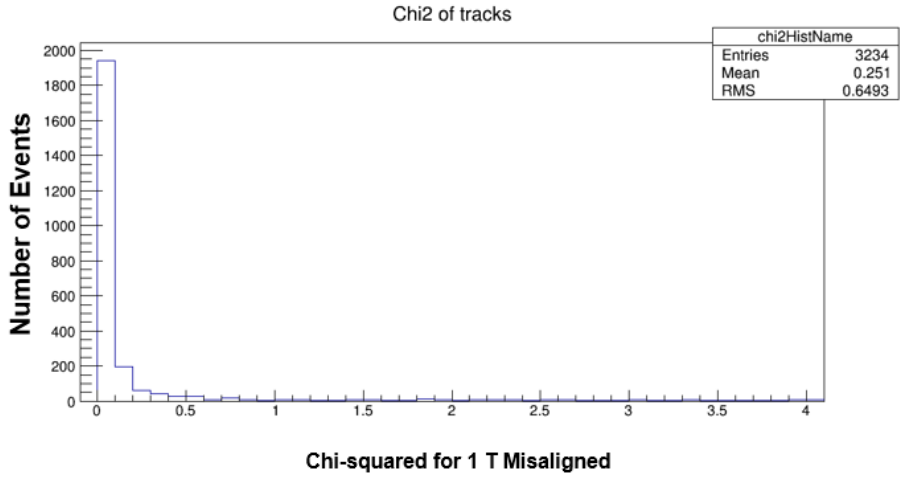

Figure 17: Finally the χ^2 for the 1 T field, with the same deviation from unity due to the misalignments of the field planes. The 0.5 T and 1 T distributions are comparatively thinner than the 0 T distribution due to the use of fewer statistics.

5.3 Zero Field Alignment: X and Y Shifts

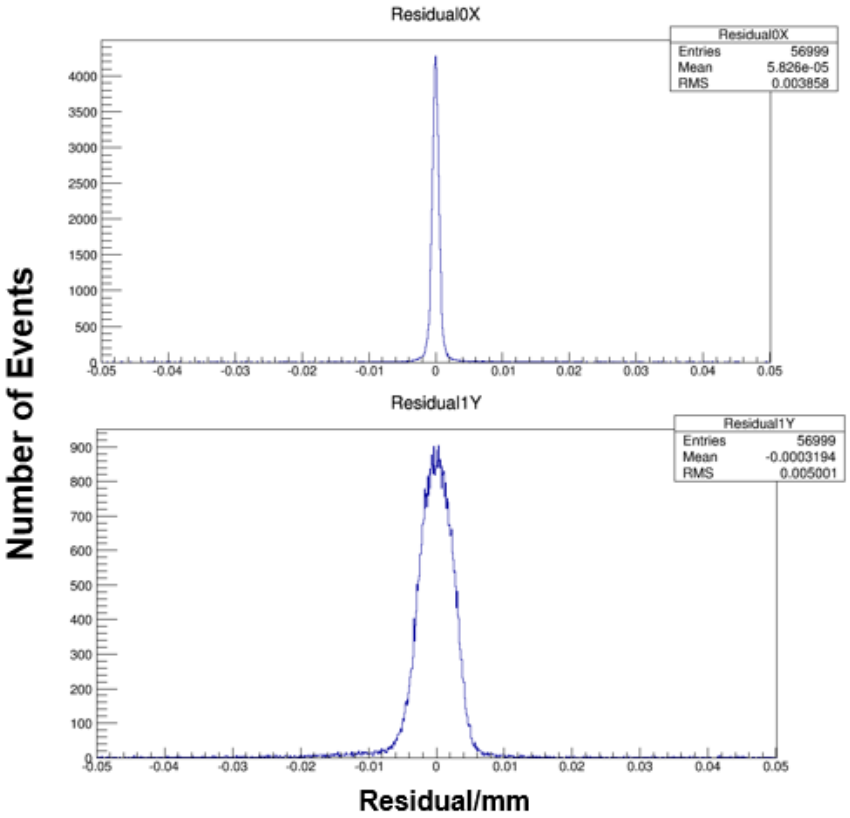

Figure 18: Example x and y-residuals for the zero field data after alignment has been applied. The residuals are now sufficiently zeroed. This is for alignment of the x and y-translations. The widths of the residuals are still significant due to the remaining misalignments, i.e. misalignments due to z-rotations. It is expected that further alignments will reduce the residual widths further.

The full iterative alignment generates residuals for the aligned tracks. Fig. 18 (above) gives the residuals in x and y for zero field after alignment. The iterative alignment was applied to align for x and y translations of the planes. The alignment should be generalised in future to align the planes for misalignments due to x, y and z-rotations. It can be seen that the alignment successfully zeroes the residuals (and differential residuals) for field-off conditions and x and y translations.

The important analysis to focus on is the aligned χ^2 distribution, given in Fig. 19. The χ^2 is now normalised to within 10 % of unity. This provides a goodness of fit which demonstrates that the track-fitted model provides a good fit of the true particle trajectory given by the hits. The alignment procedure has successfully aligned the planes in

x and y translations.

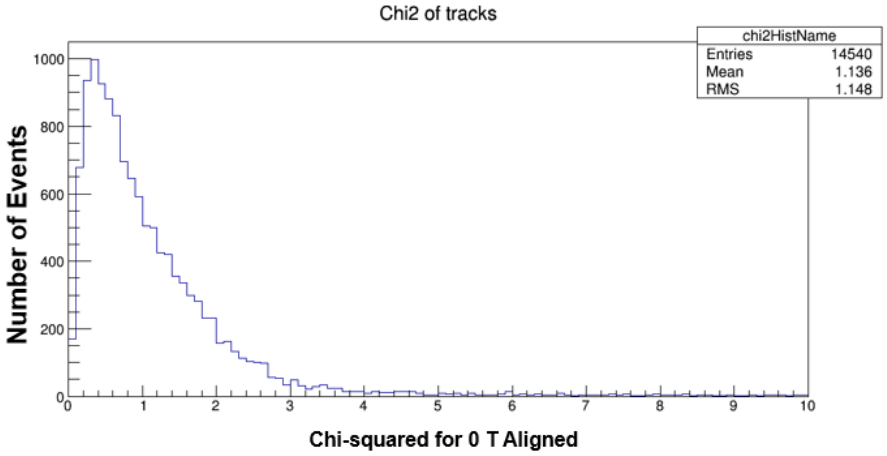

Figure 19: The new χ^2 distribution for the 0 T aligned data. The new mean value is significantly closer to unity. This indicates a far better comparison between the GBL-fitted tracks and the raw hits after the alignment procedure has been applied.

5.4 1 T Field Alignment: Asymmetries and Peaks

The 1 T field data has some interesting features. The residuals given by Fig. 20 also show x and y translation alignment. However, these residuals have significantly larger root-mean-squared width than for the case with field off. To understand what is causing this larger width, the asymmetries in the alignment must be understood.

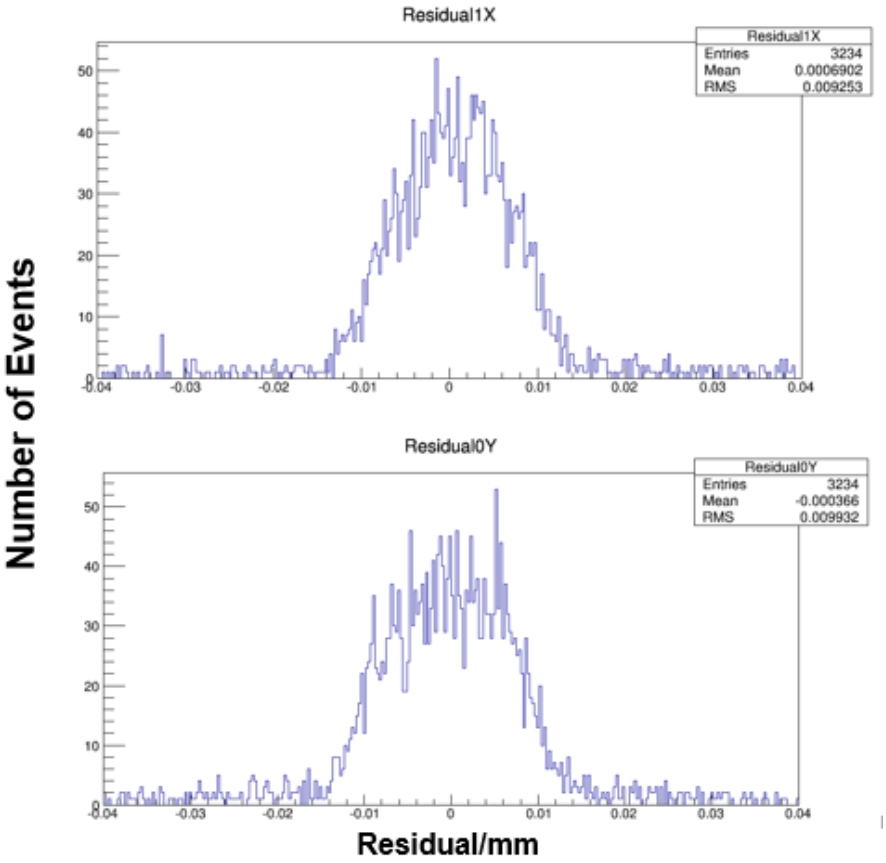

Figure 20: Example on-field residuals with large RMS values for the residuals. This is an important example of how asymmetries along the z-direction are causing larger residual errors, producing larger widths on the plots. These asymmetries due to z-misalignment shall be discussed in more detail.

Fig. 21 gives plots of the x and y-positions of the planes in the test-beam set up, as a function of the residual values at each plane. These plots are interpreted in a specific way. To establish a comparison, a) was plotted using 0 T data, and b) using 1 T data with the large RMS values.

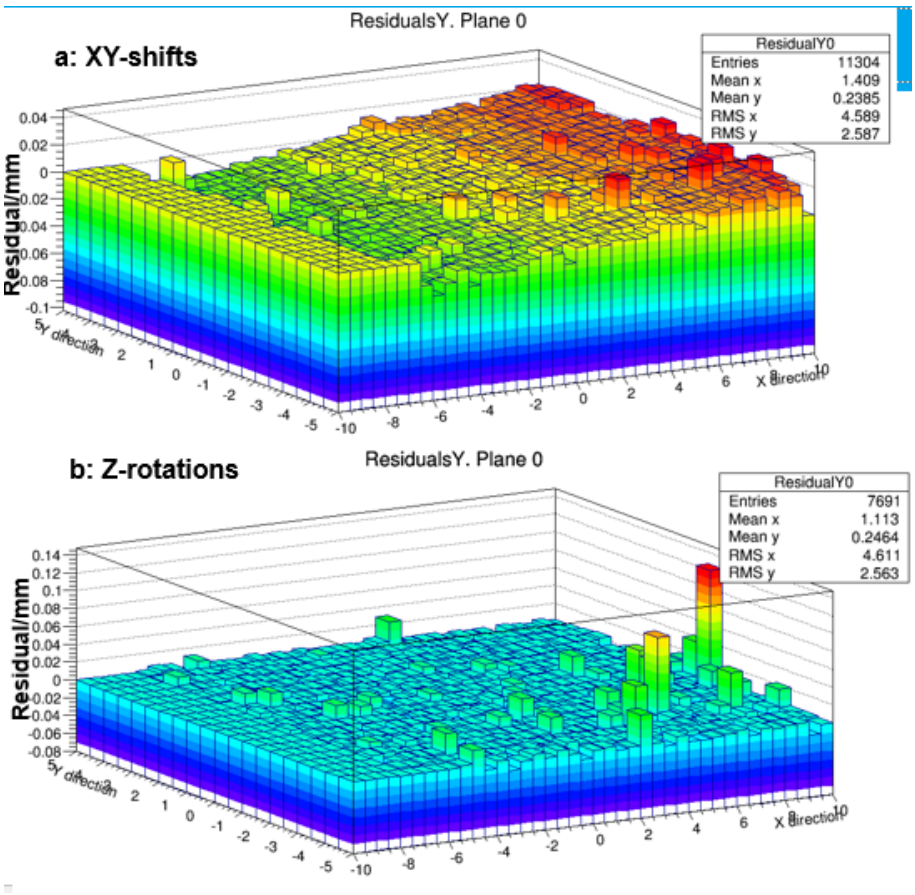

Figure 21: The x and y plane positions plotted as a function of the residuals. One plot shows a clear asymmetry in the residuals, moving along the x-axis. This asymmetry acts in the symmetry axis to x and y: the z-axis. The nature of this asymmetry is that fact that the planes have not yet been aligned in z (i.e. for z-rotations. This is compared with a data example that does not show an extreme asymmetry. This plot was taken after z-rotations had been accounted for. See the next section.

Take the x-position axis as some misaligned axis, which lies at some angle to a perfectly-aligned axis. At the origin of this coordinate system, where these two axes meet, the x-position axis corresponds to the perfect alignment. However, moving along the x, the separation between the x-position and the perfectly-aligned axis increases. This effect is responsible for the asymmetry seen in 21 b), moving along the x-position. It is this asymmetry which is producing the widths in the field-on residuals. The asymmetry is along the symmetry axis of the x-positions and the y-positions: this must be the z-position axis. Therefore, the asymmetry in the 0 T data is due to a misalignment in z. In order to take account on this asymmetry in future the alignment must be re-applied after x and y-translations have been taken account of. This second alignment must correct for z-rotations of the planes. The field-off data is not so strongly affected by these

z-rotation misalignments, as can be seen in 21 a).

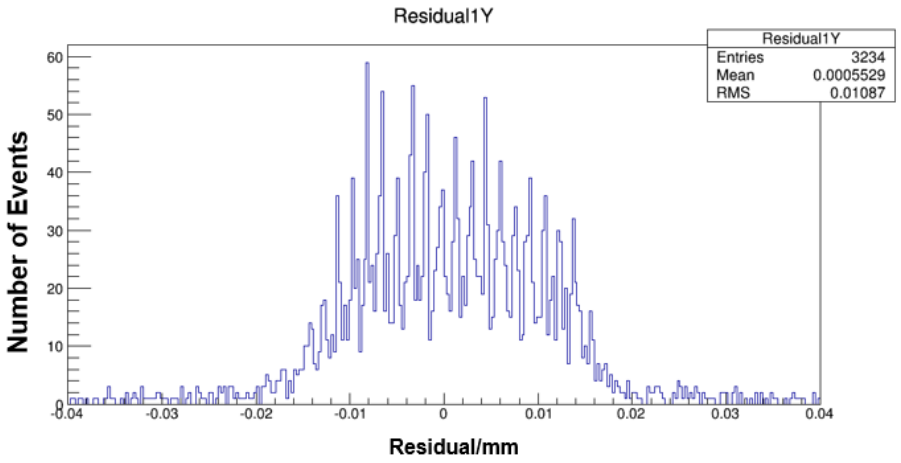

Figure 22: This is an extreme example of the peak-like substructures that are observed in some of the data. The peaks are easily seen in magnetic field data, are are typically separated by sizes of the order of a micron. The nature of these peaks is believed to be a software feature rather than being due to any actual physics.

Another striking feature of the 1 T residuals as a peak-like structure, as shown in Fig. 22 above. The reasoning behind these peaks is still not yet understood. These peaks have also been observed in zero-field data, and so cannot be due to magnetic field effects. The peaks are not due to scattering effects because these effects would be stochastic. The peaks are also not due to any rounding errors or particular binings of the plots generated. A future goal will therefore be to a) align the z-rotations to take account of asymmetries, and b) the understand the origins of these peaks in the alignment. An important step in understanding the peak data will be to study new plane geometries and different magnetic fields.

5.5 Further Residual Analysis

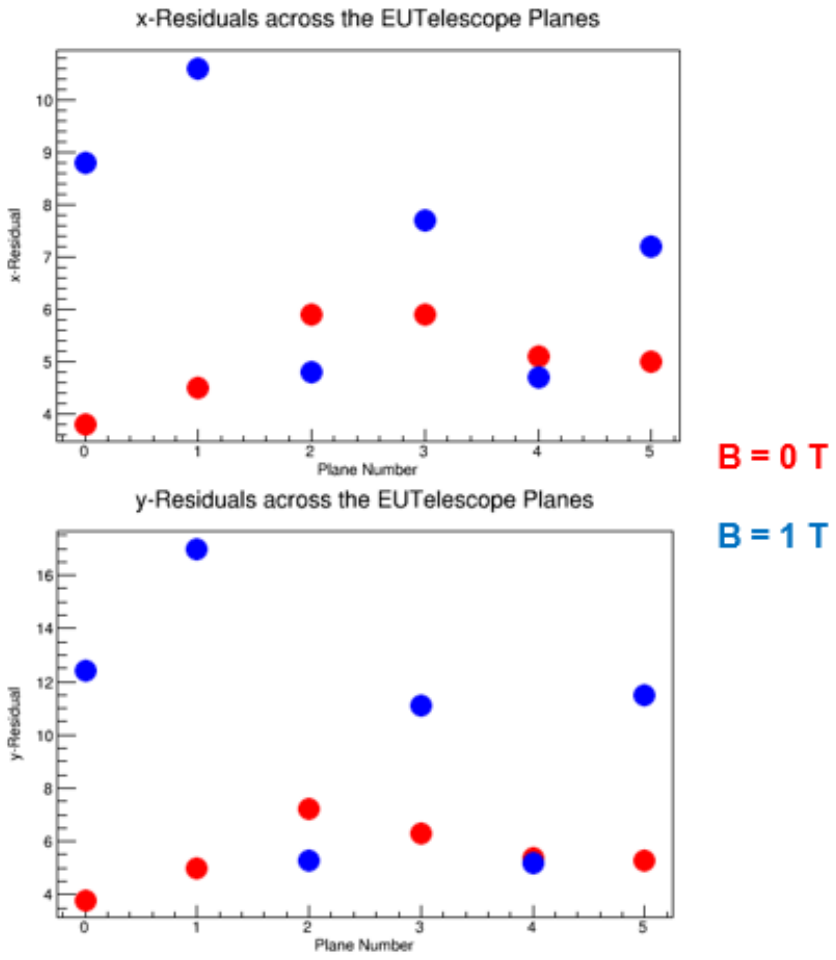

Figure 23: The raw residuals, in mm, as a function of the six planes in the EUDET.The distributions are presented for field-on and field-off. The similarity between the x and y distributions is a direct consequence of the asymmetries in the z-rotations.

A final comparison is between the x and y residuals and differential residuals. The residuals at different planes for both 0 T and 1 T data are plotted in Fig. 23. The corresponding differential residuals are given in Fig. 24.

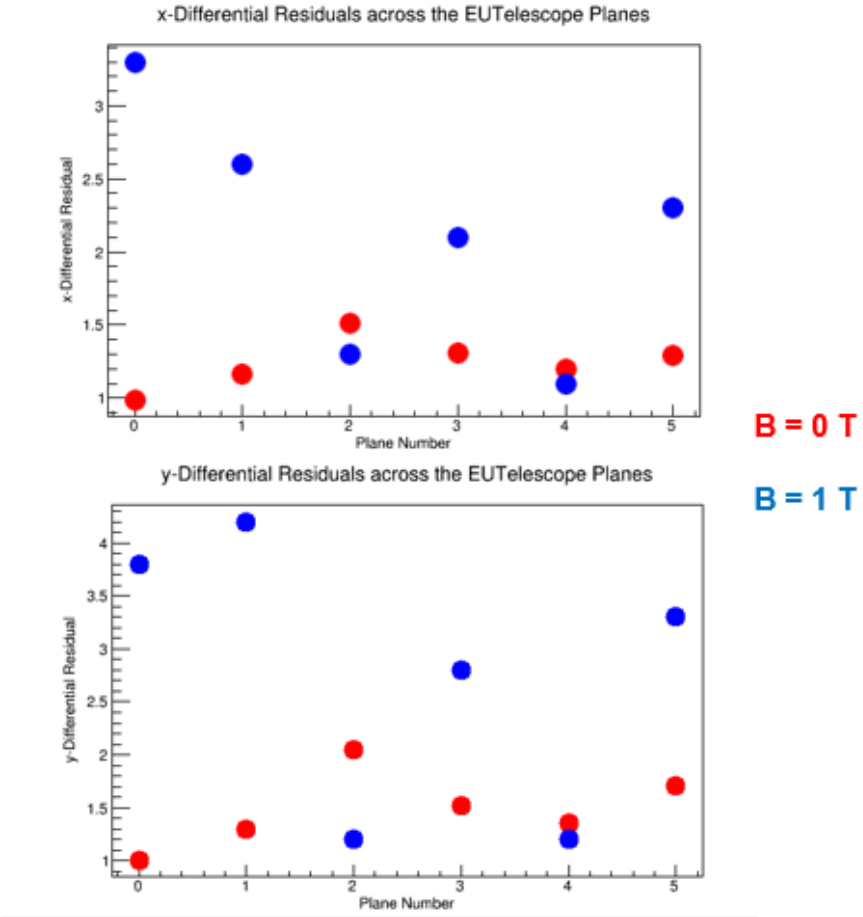

Figure 24: Corresponding differential residuals as a function of the plane number. The difference in the deviations is due to different raw errors associated with each measurement plane.

The x and y-residuals have roughly identical distributions across the 6 planes. The separate 0 T and 1 T distributions differ because different plane geometries were used for the data-taking. The same x and y distributions validate the asymmetry present due to z-rotations. The differential residual distributions in x and y are different. This is because these residuals are weighted by the errors, and the errors on each of the 6 planes will differ.

5.6 Z Rotation Alignment

The above issues with the large RMS widths in the residuals for the x and y-shift alignments are due to the misalignment about the symmetry axis shared by x and y: the z-axis. The GBL code was modified to correctly align for z-rotations. The widths in the 1 T and 0.5 T fields have been reduced by the z alignments. This demonstrates that the

initial asymmetries observed were due to misalignments in z, and can be mitigated by generalising the iterative alignment to include z-rotations. A future task will be to fully generalise iterative alignment to include also x and y-rotations and z-shifts. Further work can then begin with data for the tilted EUDET sensors.

6 Conclusions

The track reconstruction and alignment of measured particle hits on the six planes in the EUDET framework has been carried out for different environments (magnetic field 0 T and 1 T) and geometries (different plane positions and plane separations). The full process of iterative alignment successfully aligns the reconstructed tracks for cases of zero field and x and y translational misalignments. In the future it will also be necessary to align the planes in more general directions: x,y and z-rotations. Alignment using z-rotations is important because the misalignments in z-rotations introduce asymmetries in to the x and y-shift residuals. Aligning in z will remove these asymmetries.

Another unexpected feature is the presence of peaks, which are particularly prominent in the magnetic field data. To understand this it will be necessary to study different magnetic field magnitudes and different plane geometries using iterative alignment.

Overall the alignments in x and y are successful, and the alignment algorithms implemented can be applied to the alignment and calibration of important devices under test, such as the ATLAS pixel and strip detectors. Testing would talk place, for example, in the EUDET set-up at DESY, and using the 5 GeV DESY test-beam. This application will be invaluable in the near future when these detectors are being re-developed for the high-luminosity LHC upgrade.

References

[1] Recent results of the ATLAS Upgrade Planar Pixel Sensors RD Project, arXiv:1109.3047v2 (2012) *Marchiori G.*

[2] Fast alignment of a complex tracking detector using advanced track models, arXiv:1103.3909v1 (2011) *Blobel V., Kleinwort C., Meler F.*

[3] General broken lines as advanced track fitting method, arXiv:1201.4320v1 (2012) *Kleinwort C.*

[4] Track fitting and alignment for a TPC with General Broken Lines, LC-TOOL-2014-008 http://www-flc.desy.de/lcnotes (2014) *Kleinwort C.*

[5] A New Method for the High-Precision Alignment of Track Detectors, arXiv:hep-ex/0208021v1 (2002) *Blobel V., Kleinwort C.*

[6] Sensor Alignment by Tracks, arXiv:physics/0306034v2 (2003) *Karimaki V., Heikkinen A., Lampen T., Linden T.*

[7] Alignment with Tracks, VERTEX 2009 (2009) *Hulsbergen W.*